Exercise 1. Hybrid-Input-Output algorithm and Error reduction algorithm

One of the crucial problems needs to be faced in X-ray imaging is the loss of phase in the diffraction intensity, which is known as crystallographic phase problem [1]. In Miao's paper [2], they explained a feasible method to overcome this problem. They demonstrated that through oversampling the diffraction pattern and using iterative algorithms can reconstruct the image. This exercise focuses on phase retrieval algorithms, through which the provided data is reconstructed by using Hybrid-Input-Output algorithm and Error reduction algorithm [3] based on Matlab 2020b.

The provided data include given Fourier amplitude modulus in the detector $F(x)$, initial object guess $g(x)$ and an object constraint domain. The Error reduction algorithm developed from the Gerchberg–Saxton algorithm [4]. In each ER iteration, it takes four steps to process. Following is the example of the k_{th} iteration steps.
Step 1. Calculating the Furious transform of the k_{th} object guess $g_k(x)$ to get $G_k(u)$.

$$G_k(u) = |G(u)|\, e^{i\phi_k(u)} = \mathcal{F}(g_k(x)) \tag{1}$$

Step 2. Updating the real part of $G_k(u)$ with the real part of $F(x)$.

$$G'_k(u) = |F(u)|\, e^{i\phi_k(u)} \tag{2}$$

Step 3. Calculating inverse Furious transform of updated $G'_k(u)$ to get $g'_k(x)$.

$$g'_k(x) = \left|g'_k(x)\right| e^{i\theta'_k(x)} = \mathcal{F}^{-1}(G'_k(u)) \tag{3}$$

Step 4. Preparing $g_{k+1}(x)$ for next iteration. The region γ contains all the points violate the constraints. Need to note that all the $f(x)$ should be real and nonnegative, and also within the given object constraint domain.

$$g_{k+1}(x) = \begin{cases} g'_k(x), & \text{if } x \notin \gamma \\ 0, & \text{if } x \in \gamma \end{cases} \tag{4}$$

As for Hybrid-Input-Output algorithm, the first three steps are the same with the Error reduction algorithm explained above. At the final step, instead of forcing $g_{k+1}(x)$ to zero if $g'_k(x)$ violates the constraints, it makes $g_{k+1}(x) = g_k(x) - \beta g'_k(x)$ which contains feedback information from previous iteration. Here β is a feedback parameter which can take a value between 0 and 1.

$$g_{k+1}(x) = \begin{cases} g'_k(x), & \text{if } x \notin \gamma \\ g_k(x) - \beta g'_k(x), & \text{if } x \in \gamma \end{cases} \tag{5}$$

This exercise combines the Hybrid-Input-Output algorithm and Error reduction algorithm together. Each iteration contains 45 times of HIO iterations and another 5 times of ER iteration. The coding is provided in the file E1.mlx.

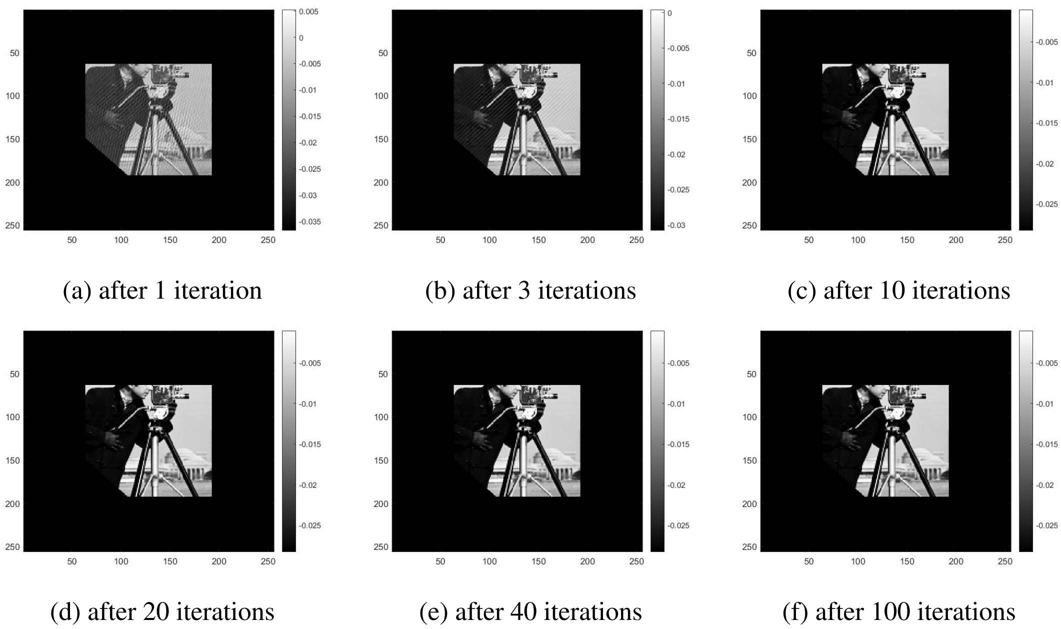

(a) after 1 iteration (b) after 3 iterations (c) after 10 iterations

(d) after 20 iterations (e) after 40 iterations (f) after 100 iterations

Figure 1: images processed by HIO phase iteration and ER algorithm

Figure 1 shows the result of this exercise. There is always a black region in each image, which is the region γ mentioned above used to remove non-object parts of the image. From Figure 1 it can be seen that after one iteration, the content of the image is discernible but not clear enough. With the increase of the number of iterations, the quality of image improves. However, by looking at the images, after 10 iterations they look very similar to each other. Here introduce the mean-squared error at each iteration can be defined in the Fourier domain [3] by

$$E_F^2 = \frac{\iint_{-\infty}^{\infty} [|G_k(u)| - |F(u)|]^2 \, du}{\iint_{-\infty}^{\infty} |F(u)|^2 \, du} \tag{6}$$

Figure 2 shows the trend of mean-squared error in the Fourier domain with increasing number of iterations, and Figure 2b is the zoom in version of Figure 2a. It is clear that the result converges after 40 iterations.

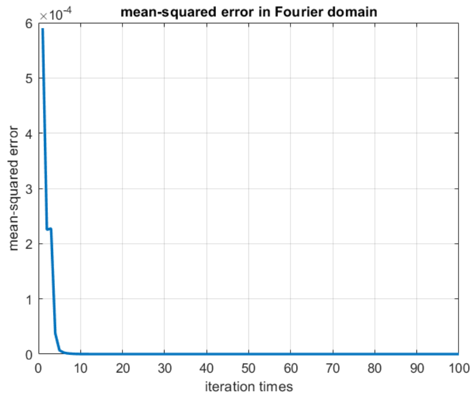

(a)

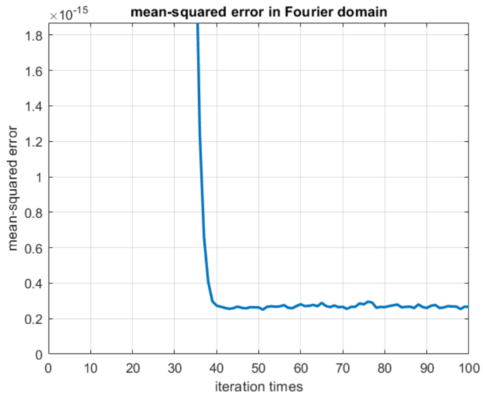

(b)

Figure 2: mean-squared error at each iteration in the Fourier domain

Exercise 2. TIE phase retrieval with Paganin algorithm

Transport-of-intensity equation (TIE) describes the intensity evolution and phase distribution of a wave on propagation [5].

$$\nabla_\perp \cdot (I(r_\perp, z) \nabla_\perp \varphi(r_\perp, z)) = -\frac{2\pi}{\lambda} \frac{\partial}{\partial z} I(r_\perp, z) \tag{7}$$

The mean idea is to solve the phase $\varphi(r_\perp, z)$ by given measurements of the intensity $I(r_\perp, z)$ and intensity derivative $\frac{\partial I(r_\perp,z)}{\partial z}$ through transport-of-intensity equation. In Paganin's paper, they demonstrated an algorithm which can be used to extract simultaneous phase and amplitude from a single defocused image of a homogeneous object [6]. Exercise 2 aims to apply the equation (10) in Paganin's paper [6], which is shown as Equation8 in this report. (The derivation is not elaborated here, the detailed process is provided in the paper.)

$$T(r_\perp) = -\frac{1}{\mu} log_e \left(\mathcal{F}^{-1} \left\{ \mu \frac{\mathcal{F}\left\{ I(r_\perp, z = R_2)/I^{in} \right\}}{R_2 \delta \left| k_\perp \right|^2 + \mu} \right\} \right) \tag{8}$$

To calculate the projected thickness $T(r_\perp)$ needs to know: the linear attenuation coefficient μ, the distance R_2, the detected intensity $I(r_\perp, z = R_2)$, the uniform intensity of the incident radiation I^{in} and the transverse momentum $k_\perp$. The tricky part is to calculate the transverse momentum. Therefore, this part refers to the method published by Diivanand Ramalingam [7] for calculating $k_\perp$. This method starting by creating axis located on the centre of the measured image and then using the coordinates to calculate the transverse momentum of each point. The coding is provided in the file E2.mlx.

Figure 3 shows the images generated by intensity detector and retrieved projected thickness. The location of different objects in these two images are the same, and similar to the examples shown in Paganin's paper [6]. Therefore, it suggests that this coding successfully calculated the projected thickness.

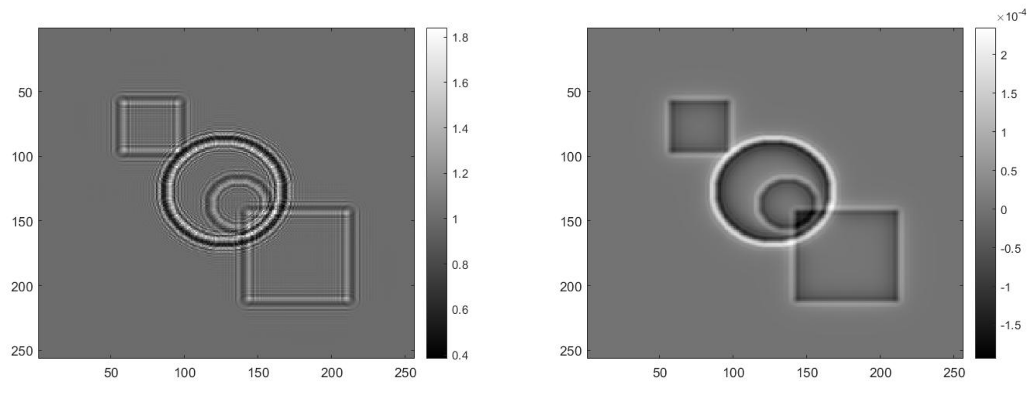

(a) image of intensity detector (b) image of projected thickness

Figure 3: retrieving projected thickness

References

[1] R. P. Millane, "Phase retrieval in crystallography and optics," *JOSA A*, vol. 7, no. 3, pp. 394–411, 1990.

[2] J. Miao, P. Charalambous, J. Kirz, and D. Sayre, "Extending the methodology of x-ray crystallography to allow imaging of micrometre-sized non-crystalline specimens," *Nature*, vol. 400, no. 6742, pp. 342–344, 1999.

[3] J. R. Fienup, "Reconstruction of an object from the modulus of its fourier transform," *Optics letters*, vol. 3, no. 1, pp. 27–29, 1978.

[4] R. W. Gerchberg, "A practical algorithm for the determination of phase from image and diffraction plane pictures," *Optik*, vol. 35, pp. 237–246, 1972.

[5] M. R. Teague, "Deterministic phase retrieval: a green's function solution," *JOSA*, vol. 73, no. 11, pp. 1434–1441, 1983.

[6] D. Paganin, S. C. Mayo, T. E. Gureyev, P. R. Miller, and S. W. Wilkins, "Simultaneous phase and amplitude extraction from a single defocused image of a homogeneous object," *Journal of microscopy*, vol. 206, no. 1, pp. 33–40, 2002.

[7] D. Ramalingam, "Xray-tie." [Online]. Available: https://github.com/Waller-Lab/Xray-TIE